COBEM 2021 26th International Congress of Mechanical Engineering
November 22-26, 2021, Virtual Congress, Brazil

COB-2021-0879
FLUID DYNAMIC STUDY IN A FLEXIBLE ARTERIOVENOUS FISTULA MODEL

Everton Guedes de Lima
Jonhattan Ferreira Rangel
Federal University of Rio Grande do Norte, Department of Mechanical Engineering, Center of Technology, Laboratory of Fluid Mechanics, Avenue Senador Salgado Filho, 300 – Lagoa Nova, CEP 59078-970 – Natal/RN
everton.gl@hotmail.com
ferreira.rangel.095@ufrn.edu.br

Alexsandra Tomé dos Santos
alexsandra__santos@hotmail.com

Willyam Brito de Almeida Santos
willyambas@gmail.com

Kleiber Lima de Bessa
klbessa@ct.ufrn.br

Abstract. *Hemodialysis is the process of extracorporeal dialysis in which the patient's blood is withdrawn through a vascular access (VA) and returned to the patient after passing through a filtration system. Among the most common accesses, the arteriovenous fistula (AVF) is recognized as the best for hemodialysis, providing a continuous and long-lasting treatment, however, it has high maturation failure rates. The present work seeks to analyze the pressure field and fluid flow conditions in a flexible arteriovenous fistula with an artery wall thickness greater than that of the vein. Through the reconstruction and treatment of the DICOM files, fabrication of the flexible AVF, adaptation of the experimental workbench and experimental procedures of the AVF, it will be possible to analyze the experimental data. The collected data were analyzed trying to establish a relationship between the pathological regions and the values in the pressure points collected from the system. Finally, it can be concluded that a wall thickness of 1 mm in the venous segment caused a pressure recovery in this segment and a high loss of load located in the region of the anastomosis was observed.*

Keywords: *Pressure, Flow rate, Wall thickness, Deformation, AVF.*

1. INTRODUCTION

Hemodialysis (HD) is a procedure performed in patients with chronic kidney failure (CKF), which consists of filtering and cleaning the blood, removing fluids and toxins. Blood is removed through a vascular access (VA), providing better conditions in the treatment of patients with CKF.

The arteriovenous fistula (AVF) is a connection between an artery and a vein commonly performed in the wrist or arm, the access is constructed through surgery by a professional in the vascular area. Thus, allowing rapid blood circulation from the artery to the vein. This rapid circulation occurs because the AVF provides a short circuit between the arterial and venous system, enabling the passage of blood through the path of least resistance (Owens & Brower, 1980). With the increase in flow in the AVF, the vessel dilates and consequently does not cause an excessive increase in shear stress. In the period of maturation, the vein is expanded, and the wall thickness is reduced, thus facilitating vascular access for HD (Sivanesan *et al*., 1999).

The AVF is the VA that has the greatest benefits when compared to other types of access. The absence of penetrating tubes and catheters on the body surface, normal use of the arm outside HD sessions, absence of dressings right after the HD section, low risk of infection and thrombosis and simple and quick access to blood circulation are advantages that make the most used AVF (Gill et al., 2017). However, the non-maturation and early failure of the AVF ranges from 40 to 60%, among the main causes is intimal hyperplasia (IH), pseudoaneurysms and stenosis (Dember, 2011). Thus, causing unfavorable clinical outcomes and significant additional costs for healthcare systems around the world.

According to Mulvany (2002) and Heagerty et al. (1993) increased intravascular pressure in patients with hypertension may cause vascular remodeling. These remodelings associated with increased pressure cause, among other things, a reduction in the elasticity of the walls that make up blood vessels.

These remodelings imply changes in the flow conditions of the system and in the vascular structure desired for the treatment or, depending on the resulting hemodynamic factors, cause unwanted pathological conditions, which depending on the severity, can lead to AVF failure and/or new surgical intervention.

The successful maturation of the AVF depends on the dilation and remodeling of the artery and vein, therefore, the more rigid vessels of patients with CKF may respond poorly to the signals that promote these adaptations (Paulson, 2014).

In order to analyze the influence of wall thickness, this work aims to understand the performance of the pressure field and flow conditions in a flexible arteriovenous fistula with variable thickness between the blood vessels that compose it.

2. METHODOLOGY

In this topic, the process of acquisition and modeling of medical data, the fabrication of the AVF and use of the workbench for the acquisition of experimental data will be addressed.

2.1 Data Acquisition and Processing

A computed tomography scan of the chest and left upper limb of the patient's brachial region was used to acquire the AVF geometry, performed at the Onofre Lopes University Hospital of the Federal University of Rio Grande do Norte (UFRN). To obtain the geometry and three-dimensional file, the InVesaliuns software (CTI Renato Archer, Campinas, SP) was used as shown in Figure 1a, and an image treatment was carried out using the Autodesk Meshmixer software (San Rafael, CA, USA) seen in Figure 1b.

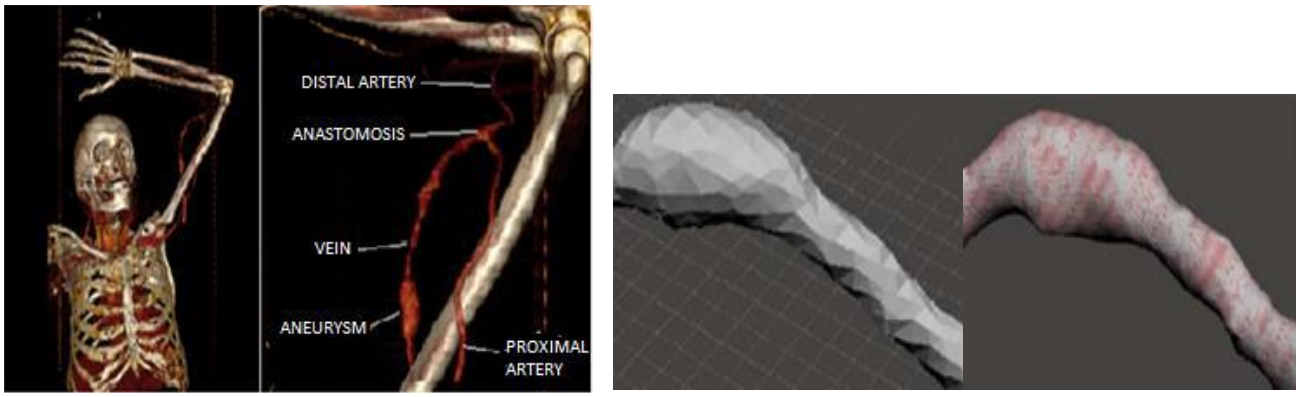

(a) (b)

Figure 1. (a) Images obtained via CT scan being processed through Invesalius; (b) Images being treated on Autodesk Meshmixer.

2.2 FAV Manufacturing

A mold from previous works was used for experiments with constant wall thickness throughout the AVF, carried out at the Laboratory of Fluid Mechanics (LMF) at UFRN. After obtaining the three-dimensional file and improving the surface, access channels were made in the Fusion 360 software (Autodesk) to collect pressure data and proximal ends for fluid inlet and outlet, resulting in a male for building an AVF model flexible 1mm thick on the venous wall and 2mm on the arterial wall, represented by Figure 2.

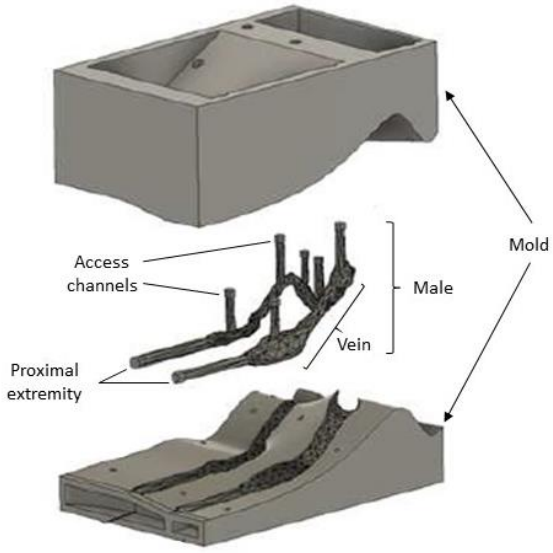

Figure 2. Representation of the male and mold for manufacturing the flexible AVF.

With the three-dimensional file of the AVF ready, 3D printing was performed using the ABS filament, spacing of 0.1 mm between the printing threads and a filling of 50% of material, resulting in better print quality and necessary rigidity.

Figure 3. 3D printing of the male for manufacturing the FAV.

To make the AVF, the male was inserted into the bipartite mold, injected with silicone rubber and allowed to cure for 24 hours. After the curing time, the AVF was removed from the mold along with the male inside it and immersed in 98% pure acetone for dismantling and removal of the ABS composite male, thus leaving only the silicone AVF model.

2.3 Experimental Workbench

The LMF experimental bench was used to promote fluid flow through the AVF and capture the pressure and flow data at established points in the system, which are illustrated in Figure 4.

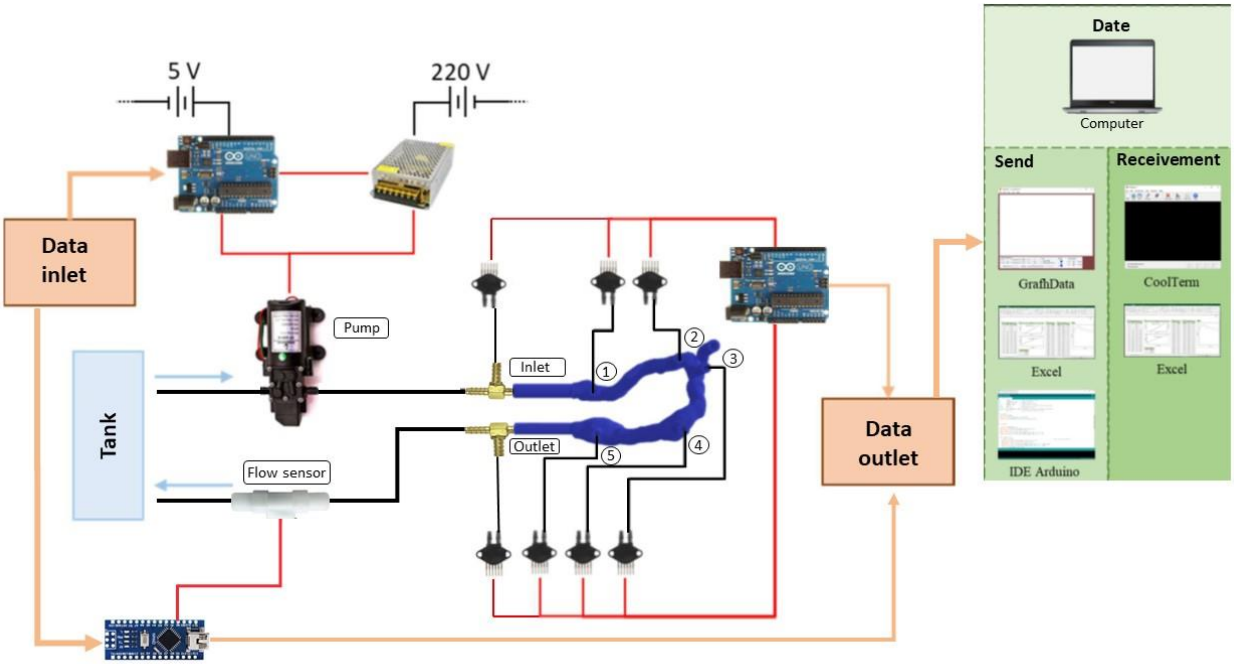

Figure 4. Schematic image of the experimental bench.

For the experiment in steady state, the load of the diaphragm pump varied from 30 to 80% of its total capacity, being increased by 5%. These parameters were used due to the impossibility of flow due to the inertia of the system for loads below 30% and the possibility of model failure for loads above 80%. The workbench contains a system for sending, receiving and storing the data necessary for operating the system.

For flow acquisition, a flow sensor (USN-HS41TA) located in the outlet pipe after the vein was used. Pressure data were measured by 7 (seven) pressure transducers (MPX5050DP) located at the inlet, (1), (2), (3), (4), (5) and outlet points, represented by Figure 5. To obtain pressure data at the AVF inlet and outlet, it was necessary to insert rigid connections at the proximal ends.

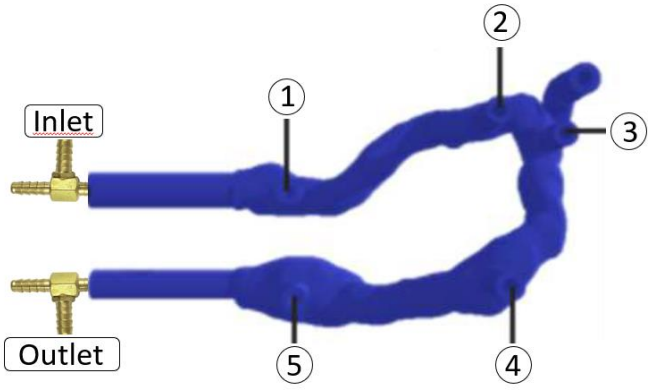

Figure 5. Schematic image of pressure tap points.

3. RESULTS AND DISCUSSION

3.1 Flexible AVF

From the acquisition, treatment, modeling and fabrication described above, the flexible AVF model was obtained, with an arterial wall thickness of 2 mm and a venous wall of 1 mm, as shown in Figure 6. After making the AVF, it was performed a visual analysis in order to find cracks and possible filling failures resulting from the manufacturing process. In this inspection process, some bubbles and filling flaws were observed, which were corrected by light painting.

Figure 6. Flexible AVF manufactured

3.2 Steady Flow

From the variation in engine load from 30 to 80%, with an increment of 5%, pressure values were obtained at the inlet points, (1), (2), (3), (4), (5) and AVF output, as a function of flow, as shown below. It should be noted that the pressure and flow range was limited by the geometry of the AVF and the load applied to the motor.

Table 1 presents the pressure and flow values with increasing motor load.

Table 1. Pressure and flow values in the flexible AVF model in kPa.

% Engine	Pressure (kPa)							Flow rate (mL/min)
	Inlet	(1)	(2)	(3)	(4)	(5)	Outlet	
30	6.9	3.8	3.2	3.3	3.2	3.2	1.6	544.5
35	8.2	5.7	5.1	4.9	5.0	5.0	2.5	759.8
40	10.6	8.0	7.3	7.2	7.3	7.3	3.9	962.0
45	12.2	10.1	9.4	8.9	9.1	9.1	4.7	1115.9
50	14.0	11.4	10.7	10.0	10.3	10.2	5.4	1226.3
55	15.6	13.1	12.3	11.3	11.9	11.9	6.1	1374.5
60	17.6	14.6	13.9	12.8	13.6	13.5	6.7	1495.1
65	19.1	16.3	15.6	14.0	15.1	15.0	7.5	1601.2
70	21.0	17.5	16.9	15.4	16.7	16.6	8.3	1697.8
75	23.2	19.5	19.0	17.0	18.3	18.1	9.3	1812.5
80	25.9	21.5	21.1	19.0	20.4	20.3	10.5	1929.7

According to Table 1, with motor load variation from 30 to 80%, inlet pressure values were obtained ranging from 6.9 to 25.8 kPa, respectively. In point (1), pressure values ranging from 3.8 to 21.5 kPa, respectively. In point (2), pressure values ranging from 3.2 to 21.1 kPa, respectively. At point (3), pressure values ranging from 3.3 to 19.0 kPa, respectively. In point (4), pressure values ranging from 3.2 to 20.4 kPa, respectively. At point (5), pressure values ranging from 3.2 to

20.3 kPa, respectively. At the outlet, pressure values ranging from 1.6 to 10.4 kPa, respectively. It can be noticed an increasing behavior of pressure in both outlets as a function of the increase in flow.

In Figure 7, the graph containing the pressure data obtained at each pressure tap is presented as a function of the flow.

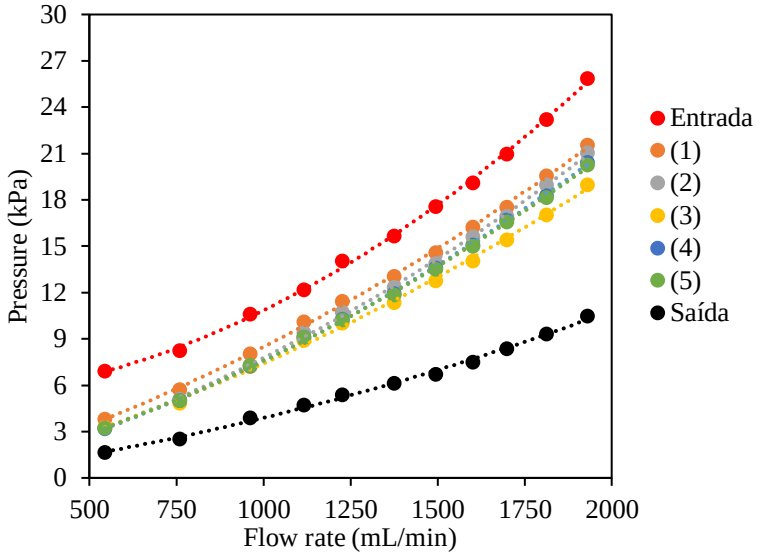

Figure 7. Pressure at collection points as a function of flow.

Analyzing the pressure values at the inlet and at point (1), there is a decrease in pressure caused by the increase in the diameter at point (1) and the damping exerted by the walls of the flexible access in the flow. Also, the highest inlet pressure values are correlated with the greatest amount of system energy located at that point.

From point (1) to (3) there is a reduction in pressure due to the loss of load distributed and located along the arterial segment. Because point (2) is located in a region with accentuated curvature, the pressure drop is also evidenced by the increase in localized pressure loss. On the other hand, the pressure drop in the anastomosis region (3), according to Botti et al. (2013), may be linked to the direction and instabilities that develop in the flow in the region of the anastomosis due to disturbances and high frequency.

After point (3), there is an increase in pressure at points (4) and (5), with the pressure of point (5) lower than that of point (4) due to the head loss existing between the two points. The increase in pressure in the venous segment may be related to the increase in the diameter of the lumen due to the reduction in the segment's wall thickness, since the smaller wall thickness in the segment makes it more flexible and provides greater vessel dilation, leading to the enlarging of the area. Shamloo et al. (2017) studied the aneurysm wall thickening effect, thereby showing that the deformation in a thicker-walled aneurysm decreased by more than 43% compared to a thinner-walled aneurysm.

Based on literature Fox et al. (2015), for the conservation of mass in incompressible fluids, when increasing the cross-sectional area, there is a reduction in the flow velocity, and the reduction in velocity leads to an increase in pressure.

It is observed that at the outlet, there is a more accentuated pressure drop due to area restriction and segment rigidity.

In Figure 8, the graph containing the pressure data obtained at points (3), (4) and (5) as a function of the flow is presented.

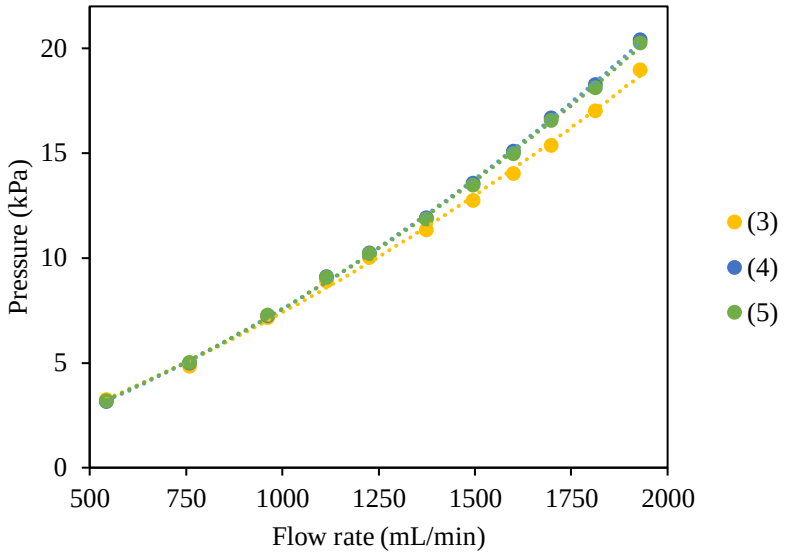

Figure 8. Pressure at points (3), (4) and (5) as a function of flow.

Analyzing the pressure data in points (3), (4) and (5), it is observed that with the increase in flow, there is a greater pressure differential. Analyzing the pressure differential between points (4) and (3), it appears that for a flow rate of 544.5 mL/min the pressure differential is -0.1 kPa, and for a flow rate of 1929.7 ml/min is 1.4 kPa. The pressure differential between points (5) and (3), for a flow rate of 544.5 mL/min is -0.1 kPa, and for a flow rate of 1929.7 mL/min it is 1.3 kPa. Thus, the increase in the pressure differential with the increase in flow is related to an increase in the area due to the greater elasticity of the venous segment, which provides a greater rate of deformation with the increase in flow. Another important factor to be analyzed is the sudden change in flow due to geometry. The flow, after the abrupt change in the vessel due to the aneurysm, forms regions of recirculation close to the walls, as shown by Bessa et al (2009).

In Figure 9, the flow and pressure differential graph as a function of the engine load percentage in the AVF is presented.

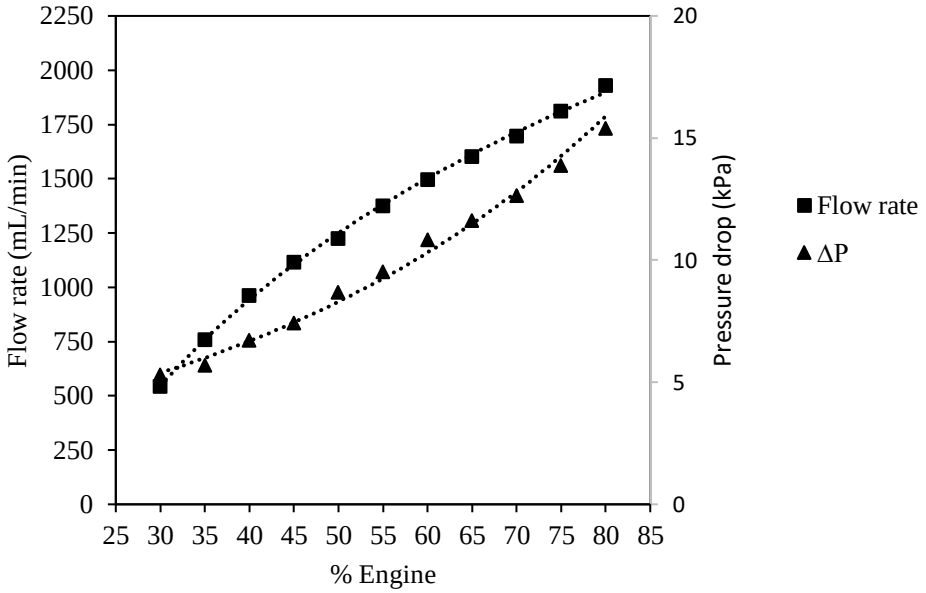

Figure 9. Flow and pressure differential as a function of the engine load percentage in the AVF.

According to the data presented, it is observed that as the engine load increases, the flow curve presents a decreasing rate, and the pressure differential presents an increasing rate. Thus, by submitting the system to higher engine loads, the FAV would reach its maximum deformation, which would lead to a constant flow with the increase in the engine load and an exponential increase in pressure drop. However, loads greater than 80% may lead to AVF rupture.

All measured pressure data had a measurement uncertainty of ±2.5%, considering the approximate uncertainty contained in the MPX5050DP sensor datasheet. As for the flow data, the error is approximately ±5%, also considering the uncertainty present in the datasheet of the USN-HS41TA sensor.

4. CONCLUSION

From the data presented, it can be concluded that a wall thickness of 1 mm in the venous segment caused a pressure recovery in points (4) and (5) located in this region. As well, there is a high loss of head located in the region of the anastomosis. Finally, we emphasize the importance of subsequent studies to correlate the influence of these hemodynamic factors on vascular pathologies and to study the reduction of load loss located in the anastomosis.

5. REFERENCES

Bessa, K. L.; Ortiz, J. P., 2009. "Flow visualization in arteriovenous fistula and aneurysm using computational fluid dynamics". *Journal of Visualization*, Vol. 12, No. 2, pp. 95–107.

Botti, L. et al., 2013. "Numerical Evaluation and Experimental Validation of Pressure Drops Across a Patient-Specific Model of Vascular Access for Hemodialysis". *Cardiovascular Engineering and Technology*, Vol. 4, No. 4, pp. 485–499.

Dember, L, M:, 2011. "Fistulas First-But Can They Last?". *Clinical Journal of the American Society of Nephrology*, Vol. 6, pp. 463-464.

Fox, R. W., Mcdonald, A., Pritchard, P., 2015. *Introdução à Mecânica dos Fluidos. 6. ed*. [s.l.] LTC - Livros Técnicos e Científicos Editora LTDA.

Gill, S.; Quinn, R., Oliver, M., Kamar, F., Kabani, R., Devoe, D., Mysore, P., Pannu, N., Macrae, J., Manns, B., Hemmelgarn, B., James, M., Tonelli, M., Lewin, A., Liu, P., Ravani, P., 2017. "Multi-disciplinary vascular access care and access outcomes in people starting hemodialysis therapy". *Clinical Journal of the American Society of Nephrology*, Vol. 12, No. 12, pp. 1991–1999.

Heagerty, A. M. et al., 1993. "Small artery structure in hypertension: Dual processes of remodeling and growth". *Hypertension*, Vol. 21, No. 4, pp. 391–397.

Mulvany, M. J., 2002. "Small artery remodeling and significance in the development of hypertension". *News in Physiological Sciences*, Vol. 17, No. 3, pp. 105–109.

Owens, M.L., Bower, R.W., 1980, "Physiology of arteriovenous fistulas", In: Wilson SE, Owens ML, eds. Vascular Access Surgery. Year Book Medical Publishers, Chicago, pp. 101-114.

Paulson, W.D., 2014. "Does Vascular Elasticity Affect Arteriovenous Fístula Maturation?". *The Open Urology & Nephrology Journal*, Vol. 7, pp. 26-32.

Shamloo A., Nejad M. A., Saeedi M., 2017. "Fluid-structure interaction simulation of a cerebral aneurysm: effects of endovascular coiling treatment and aneurysm wall thickening". *J. Mech. Behav. Biomed. Mater*. Vol. 74, pp. 72-83.

Sivanesan, S., How, T.V., Bakran, A., 1999, "Characterizing flow distributions in AV fistulae for haemodialysis access", *Nephrology Dialysis Transplantation*, Vol. 13, pp. 3108-3110.

6. RESPONSIBILITY NOTICE

The author(s) is (are) the only responsible for the printed material included in this paper.